Int. J.Nano Dimens. 5(3): 267-272, Summer 2014
ISSN: 2008-8868

Contents list available at **IJND**

International Journal of Nano Dimension

Journal homepage: *www.IJND.ir*

Determination of porous Silicon thermal conductivity using the "Mirage effect" method

F. Alfeel*
F. Awad
F. Qamar

Department of Physics, Science Faculty, Damascus University, Syria.

Received 10 April 2013
Accepted 28 June 2013

ABSTRACT

Mirage effect is contactless and non destructive method which has been used a lot to determine thermal properties of different kind of samples , transverse photothermal deflection PTD in skimming configuration with ccd camera and special programs is used to determine thermal conductivity of porous silicon ps film. Ps samples were prepared by electrochemical etching. Thermal conductivity with porosity changing was measured and the experiments result compared with theoretical results, and they were almost the same.

Keywords: *Mirage effect; Non destructive method; Photothermal deflection PTD; Thermal conductivity; Porous Silicon; Electrochemical etching; Nano Crystalline; Film.*

INTRODUCTION

When an intensity-modulated beam of electromagnetic radiation is incident on an absorbing medium, heat pulses are produced in the sample. The thermal wave thus generated diffuses into the sample as well as the adjacent coupling medium resulting in a modulated temperature gradient. Concomitant with this temperature gradient is a refractive index gradient established in the sample and in the coupling medium. The refractive index gradient leads to deflection of another optical beam (probe beam) passing through its vicinity. In the mirage detection technique, the probe beam could be directed onto the sample surface in two ways: namely bouncing configuration and skimming configuration. In the former case, the probe beam is incident at a small angle on the sample surface and is reflected. Thus the height of the probe beam above the sample surface is zero. In the skimming configuration, the probe beam grazes the sample surface. Hence, the probe beam is propagating at a finite height above the surface, which is determined by the spot size of the beam. The deflection, detected using suitable position sensitive detectors, comprises of two components— one parallel tangential component) and the other perpendicular (normal component) to the sample surface. The present theoretical analysis applies to experiment performed in skimming configuration [1].

* Corresponding author:
Faten Alfeel
Department of Physics, Science Faculty, Damascus University, Syria.
Tel +96 3944682910
Fax +96 311 33923485
Email *fatenfeel@gmail.com*

EXPERIMENTAL

Model

In order to use PDS to extract useful information about a material's properties, it is necessary to have a suitable model of heat transfer in the solid and gas phases. The following assumptions are made in the present studies in [2, 3]: transverse PDS in a Skimming probe beam configuration (Figures 1a & 1b), a multilayered material structure (Figure 1b), axi-symmetric heat flow, homogeneous density and specific heat within each layer, anisotropic thermal conductivity within each layer, a thermal contact resistance at each interface, temperature invariant properties, volumetric Optical-to-thermal energy conversion, periodically modulated heating beam, and Gaussian (TEM00) heating and probe beams.

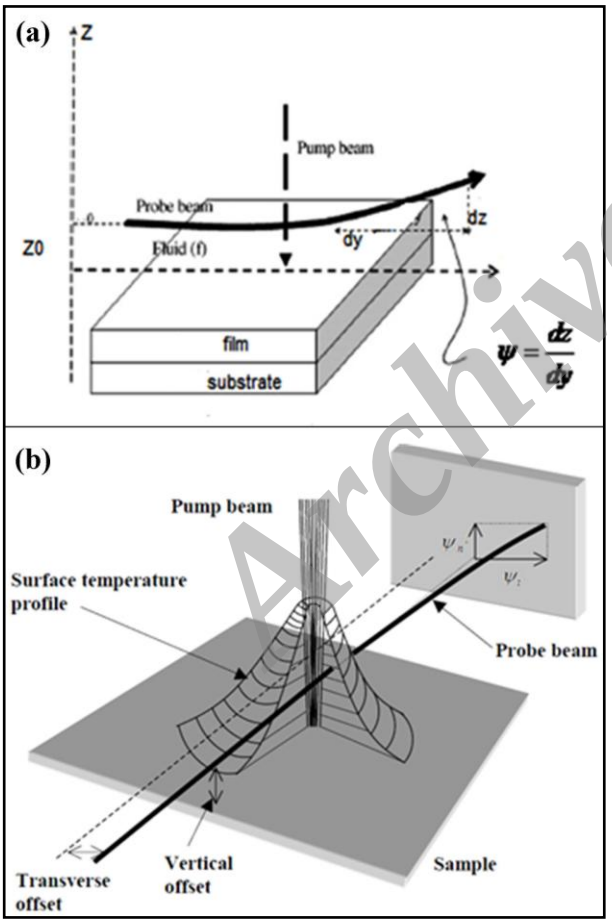

Fig. 1. Profile and the resulting normal and transverse components of the PTD signal.
(a) schematic representation of the probe beam deflection[16]
(b) schematic diagram of the passage of a probe-beam through a refractive index[2]

We will calculate the probe beam deflections caused by the temperature field determined by the following equation [2, 3, 4, 5, and 6]:

$$\nabla^2 T_0(r,z,t) = \frac{\rho_0 c_0}{\kappa_0}\frac{\partial T_0}{\partial t} \qquad (1)$$

$$\nabla^2 T_1(r,z,t) = \frac{\rho_1 c_1}{\kappa_1}\frac{\partial T_1}{\partial t} - \frac{Q(r,z,t)}{\kappa_1} \qquad (2)$$

$$\nabla^2 T_2(r,z,t) = \frac{\rho_2 c_2}{\kappa_2}\frac{\partial T_2}{\partial t} \qquad (3)$$

Where Q(r,t) is the heat deposited per unit volume oscillating at the frequency *w* in the absorbing medium and is given by [7] :

$$Q(r,z,t) = \frac{4p\alpha}{\pi^2 b^2}\exp(-\alpha z)\exp(\frac{-2r^2}{b^2})[\cos(\omega t)] \qquad (4)$$

For square wave intensity modulated beam where P is the optically exciting beam (pump beam) power, α is the absorption coefficient, and b is the l/e^2 radius of the *Gaussian beam.*

The deflection of a single ray, which is parallel to the sample surface, can be broken into orthogonal components which are normal and tangential to the surface. Where the normal and tangential components are given by [8]:

$$\psi = \frac{1}{n}\frac{\partial n}{\partial T}\int_{path}\nabla_s T(r,t)ds \qquad (5)$$

$$\psi = \psi_n + \psi_t \qquad (6)$$

$$\psi_t = \frac{1}{n_0}\frac{dn}{dT}\int_{y=-\infty}^{+\infty}\frac{\partial T_f}{\partial x}dy \quad , \quad \psi_n = \frac{1}{n_0}\frac{dn}{dT}\int_{y=-\infty}^{+\infty}\frac{\partial T_f}{\partial z}dy \qquad (7)$$

The periodic heat flow from the solid to the surrounding gas produces a periodic temperature variation in the gas. The time dependent component of the temperature in the gas attenuates rapidly to zero with increasing distance from the surface of

the solid. The Thermal length and thermal wavelength can be written as [9]:

$$\mu_i = \frac{1}{\mathrm{Re}\,\beta_i} = \sqrt{\frac{2D_i}{\omega}} \qquad (8)$$

$$\lambda_i = \frac{2\pi}{\mathrm{Im}\,\beta_i} = 2\pi\sqrt{\frac{2D_i}{\omega}} \qquad (9)$$

We can find thermal conductivity from equations (10) and (11) by solving equations (7) as in [10]:

$$\psi_n = \frac{1}{n_0}\frac{dn}{dt}\frac{I_0}{\alpha b\kappa}\sqrt[4]{b^4 + \frac{D_S^{\,2}}{\pi^2 f^2}}\exp\left[-z_0\frac{\sqrt{2}}{2}\sqrt{\frac{\pi f}{D_f}}\right] \qquad (10)$$

$$\psi_t = \frac{1}{n_0}\frac{dn}{dt}\frac{I_0}{\alpha\kappa}\exp\left[-z_0\frac{\sqrt{2}}{2}\sqrt{\frac{\pi f}{D_f}}\right] \qquad (11)$$

Where [11]:

$$\frac{dn}{dt} = \frac{-(n-1)}{T} \qquad (12)$$

n refractive index of fluid, T temperature, D_i thermal diffusivity of medium i (i=s for sample , f for fluid ,b for back), f modulation frequency of pump beam . K Thermal conductivity, α is the absorption coefficient, I_0 is the energy absorbed by the target due to the reflection of radiation from the microscopic stage, b is the $\frac{1}{e^2}$ of radius of the Gaussian beam distribution. We will assume that the probe beam is collimated in the region of the thermal field. We have solved for the intensity-averaged probe beam deflections at a particular harmonic induced by the temperature field in the gas phase. ccd camera is used instead of quadrant photo detector, we've created suit of programs that can work as beam profiler according to next step:

1. Video of the laser probe beam moving is recorded with ccd camera during heating of ps sample by pump beam.
2. The video is cut to frames (Figure 2)
3. We use program that determines the laser beam spot displacement in normal and tangential direction (Figure 3).
4. The value of displacement is used to calculate the effective thermal conductivity from equation(9,10) of the sample, and by using effective medium approximation, thermal conductivity of porous silicon film is calculated from eqs.(13,14) [12]:

$$\kappa_{eff} = \frac{L\kappa_1\kappa_2}{\kappa_1 L_2 + \kappa_2 L_1} \qquad (13)$$

$$\kappa_1 = \kappa_{eff}\frac{\kappa_2 L_1}{\kappa_2 L - \kappa_{eff} L_2} \qquad (14)$$

Where K_1 is thermal conductivity of porous silicon, K_2 thermal conductivity of silicon (150w/mk) , K_{eff} the effective thermal conductivity, L_1 the porous silicon film thickness, L_2 the silicon substrate thickness , L thickness of porous silicon film and silicon substrate together (0.4 mm).

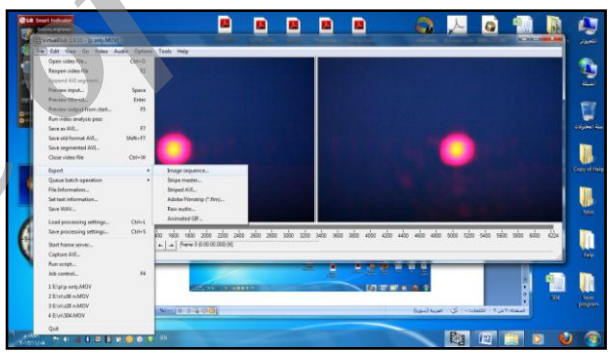

Fig. 2. Video cutting into photos every 25 frames (4s)

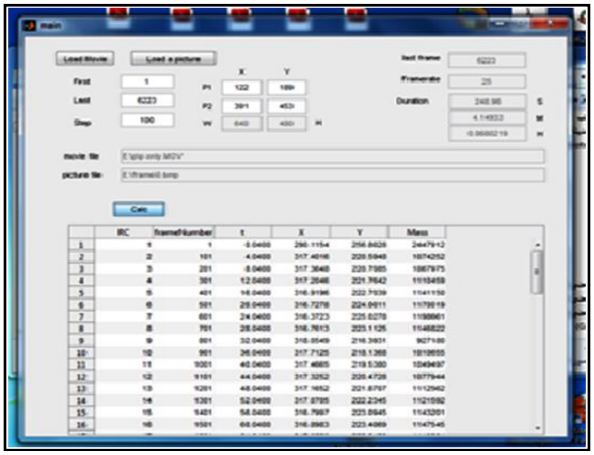

Fig. 3. program for determining of laser beam spot displacement in normal and tangential direction with time.

Fabricating process

Porous silicon samples were prepared by electrochemical etching method of p-type cubic silicon wafers (c-Si), (100) orientation with resistivity of 0.01-40 Ω·cm, electrochemical dissolution of Si wafers is used: HF-ethanol (measured by volume) aquas with concentration from 20% (Table 1). The current density was always kept Constant for each sample during etching of PS (10-50 mA/cm^2).Fabricating process done in a normal etching Teflon cell. After anodization, PS samples are carefully removed from the bath and cleaned in deionized water. Few examples of AFM measurement is presented to show differences between samples according to preparing current (Figure 4):

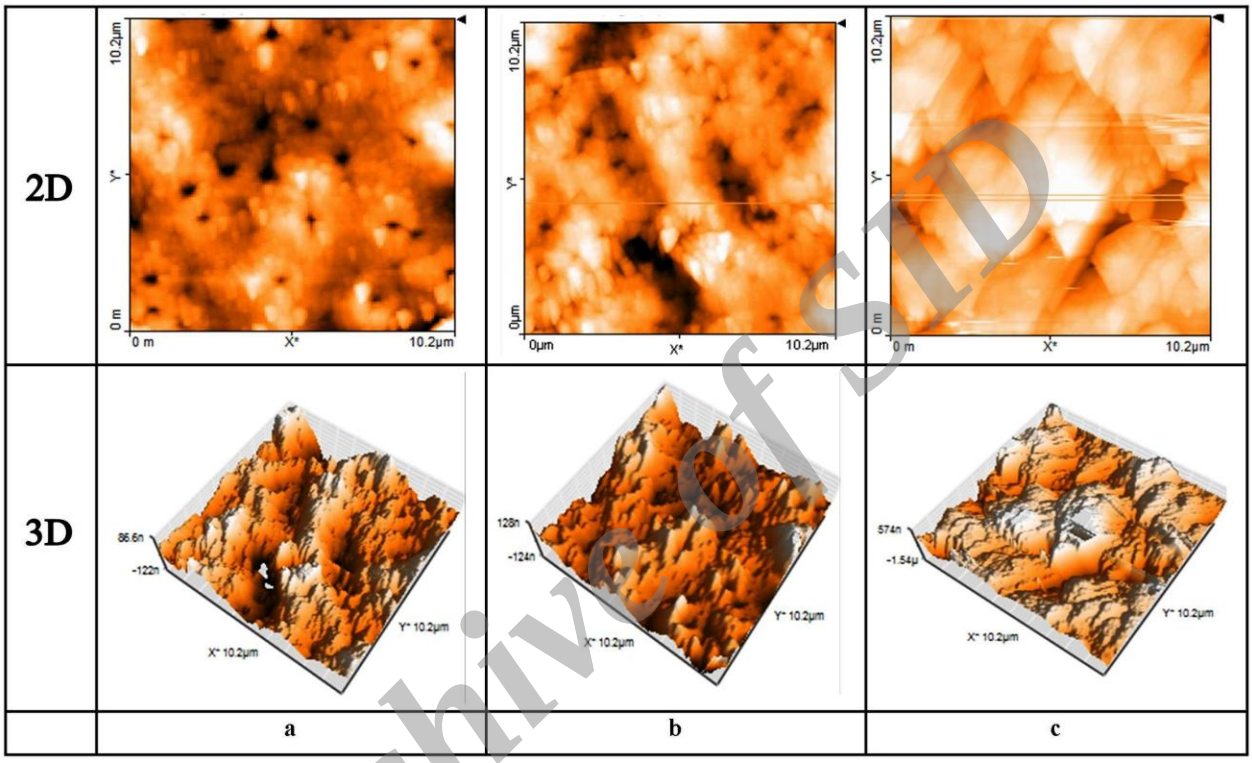

Fig. 4. 2D and 3D AFM image of porous silicon samples prepared with etching time of 5 min and current density of (a-20,b-30,c-45) mA·cm^{-2}, at HF concentration 20%.

Table 1. Fabricating process parameters

Sample	HF concentration (%)	Current density (mA/cm^2)	Anodization Time (min)
S01	20	10	5
S02	20	20	5
S03	20	25	5
S04	20	30	5
S05	20	35	5
S06	20	40	5
S07	20	45	5
S08	20	50	5

RESULTS AND DISCUSSION

Effective Thermal conductivity is plotted in Figure 5 versus porosity for samples in Table 1. Calculated from photothermal deflection method using experimental results and by substituting it in eq.(10,11) to find effective thermal conductivity then by substituting effective thermal conductivity in eq.(13,14) to find the Thermal conductivity of ps film (Table 2). It was found that the Thermal conductivity of ps film decreases with increasing porosity. The measured thermal conductivities, ranging from 92 W/mK for P=15% to 13.7 W/mK for P=55%. The thermal conductivity K_{bulk}=150W/mK of bulk Si However, our measurement results was close to theoretical results predicted by Eq. (15) [13, 14]:

$$\kappa_{1th} = \kappa_{si}(1-p)^3 \qquad (15)$$

The decreasing in Thermal conductivity is attributed to that: The solid contribution is normally significantly higher than that of the gas contained in the pores, and thus, the gaseous conduction contribution is considered to be negligible. The radiative contribution, k_{rad}, is derived from heat radiated throughout the pores, and is highly dependent on the porosity, pore size, and temperature [15]. For all that reasons thermal conductivity in bulk silicon is higher than that of ps samples. Figure 6 shows the measured and theoretical calculated thermal conductivity of ps sample they are almost the same.

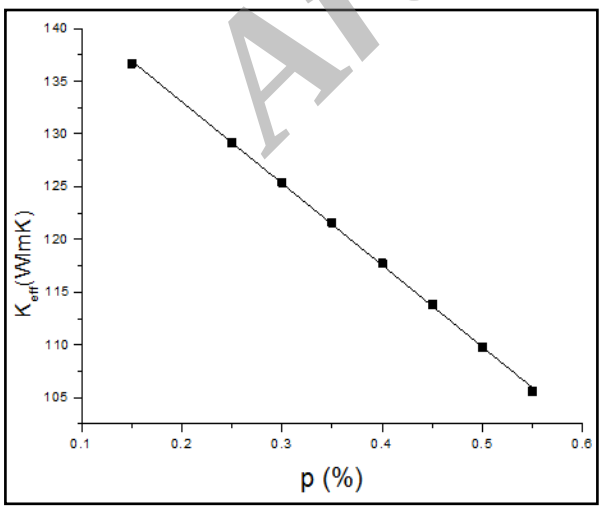

Fig. 5. The effective thermal conductivity changes vs porosity

Table 2. Thermal conductivity of ps measured and calculated

sample	p%	K_{eff} w/mK	κ_1 w/mK	$\kappa_{1theo.}$ w/mK
S01	0.15	136.7	92.1	92.2
S02	0.25	129.2	63.3	65.5
S03	0.3	125.4	51.5	51.5
S04	0.35	121.6	41.2	41.2
S05	0.4	117.7	32.4	32.4
S06	0.45	113.8	25.0	25.0
S07	0.5	109.8	18.8	18.8
S08	0.55	105.6	13.7	13.7

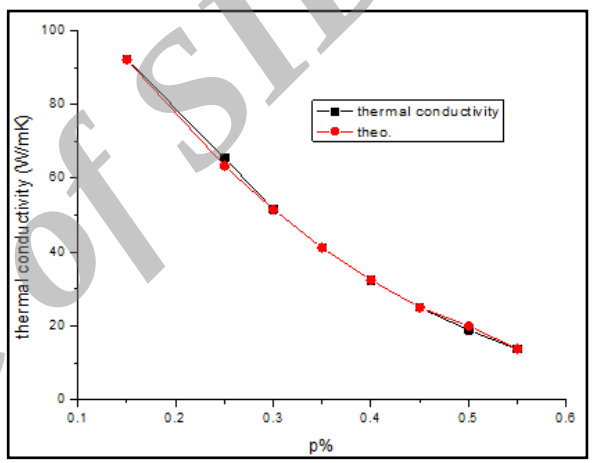

Fig. 6. The thermal conductivity of ps changes vs porosity

CONCLUSIONS

Porous silicon samples were prepared by electrochemical etching method, HF-ethanol concentration from 20%, The current density was (10,.., 50 mA/cm^2). Fabricating process done in a normal etching Teflon cell. Mirage effect in transverse photothermal deflection PTD (skimming configuration) with ccd camera and special program is used here to determine effective thermal conductivity from displacement in eq.(10,11), and by substituting them in eq.(13,14) it's easy to determine thermal conductivity of ps samples. They changed from92.1W/mK for 0.15% porosity to 13.7W/mK for 0.55% porosity. Experimental results of ps thermal conductivity with porosity were compared with theoretical results and it was almost the same.

REFERENCES

[1] Jyotsna Ravi., S. Lekshmi, K.P.R. Nair, T.M.A Rasheed,(2004) ,A simple theoretical extension to the analysis of photothermal deflection signal for low thermal diffusivity evaluation , *J.Quant. Spect.&.Rad.Transfer* 83:193–202.

[2] Nibu A.George, (2012), Estimating the thermal properties of thin film and multilayer structures using photothermal deflection spectroscopy , Thesis submitted Presented to the in Partial Fulfillment of the Requirements for the Degree of Doctor of Philosophy, Faculty of the Graduate School of Cornell University .

[3] Beaudoin, M., Chan, I.C.W., Beaton, D., Elouneg-Jamroz, M., Tiedje b, T., Whitwick, M., et.al, (2009), Bandedge absorption of GaAsN films measured by the photo- thermal deflection spectroscopy, *J.Cryst.Growth* 311:1662–1665.

[4] Jeona, P.S., Kima, J.H., Kimb, H.J., Yoob, J., (2008), Thermal conductivity measurement of anisotropic material using photothermal deflection method, *Thermochim.Acta* 477:32–37.

[5] Gotter, B., Faubel, W., Neubert , R.H.H., (2010), Photothermal imaging in 3D surface analysis of membrane drug delivery , *Europ.J.Pharm. Biopharmac*.74:26–32.

[6] Annelise During, Caroline Fossati, Mireille Commandr, (2004),Photothermal deflection microscopy for imaging sub-micronic defects in optical materials, *Opt. Commun.* 230:279–286.

[7] Jackson, W. B., Amer, N. M., Boccara, A. C., Fournier, D.,(1981), Photothermal deflection spectroscopy and detection, *Appl. Opt.*20:1333-44 .

[8] Nibu A. George, (2012), Photoacoustic and photothermal deflection studies on selected photonic materials, Thesis submitted in partial fulfilment of the requirements for the degree of doctor of philosophy, International school of photonics cochin university of science and technology, *Cochin* 682022,india

[9] Soltanol, M., Kotabi, M, and Naderi, M.H.,(2004),Three dimensional photothermal deflection and lensing in solids :the effect of modulation frequency, *Jap.J.Aappl.Phys*.43:611-620.

[10] Boubaker, K., (2006), Characterization of Metallic Atomic Structures Using the Mirage Effect, *Phys.Metals and Metallogr.* 101:45–51.

[11] Jonathan D. Spear, Richard E. Russo, and Robert J. Silva1,(1990), Collinear photothermal deflection spectroscopy with light-scattering samples, *Appl.Opt.*29:4225-34.

[12] Shen Qing and Toyodaa Taro,(2003), Dependence of thermal conductivity of porous silicon on porosity characterized by Photoacoustic technique, *Rev.Scien. Instrum.*74:848-853.

[13] Wolf, A., Brendel, R., (2006),Thermal conductivity of sintered porous silicon films, *Thin Sol.Films* 513:385–390.

[14] Alvarez, F. X.,Jou, D., and Sellitto, A., (2010), Pore-size dependence of the thermal conductivity of porous silicon: A phonon hydrodynamic approach,*Appl. Phys.Lett*.97:033103(3pages).

[15] Pappacena, K. E. and Faberw, K. T. ,(2007),Thermal Conductivity of Porous Silicon Carbide Derived from Wood Precursors, *J.A.Ceram.Soc*.90:2855-2862.

[16] Ghrib, T.,Yacoubi, N., Saadallah, F.,(2007), Simultaneous determination of thermal conductivity and diffusivity of solid samples using the “Mirage effect” method, *Sen. and Actuat.A.*135:346–354.

Cite this article as: F. Alfeel *et al.*: Determination of porous silicon thermal conductivity using the “Mirage effect” method.
Int.J.Nano Dimens. 5(3): 267-272, Summer 2014